

## TARGET SPALLATION INDUCED BY CURVED LOW $L/D$ PENETRATORS

M. Maysel<sup>1</sup>, E. Muzychuk<sup>2</sup>, E. Zaretsky<sup>3</sup>

<sup>1</sup> IMI, Central Laboratory, P.O.B 1004 Ramat Hasharon 47100, Israel

<sup>2</sup> IDF, Mil. P.O.B 01154, Israel

<sup>3</sup> Department of Mechanical Engineering, Ben-Gurion University, P.O.B. 653 Beer-Sheva 84105, Israel

The impact of three shapes of 6061-T6 aluminum projectiles was studied: planar, concave and convex. Target damage induced by the impact was examined, experimentally as well as numerically, for a range of impactor curvature radius and thickness. The projectiles were launched by a gas gun, and the back surfaces of the targets were monitored by a VISAR. The results obtained are presented. One of the main results is that the maximum target thickness, at which spall fragmentation detaches from the back surface, depends on the radius of curvature of the impactor and its thickness. Concave impactors can cause spall in thick targets due to the converging shock flow, while convex impactors cause mainly internal undetached spalls to targets of the same thickness.

### INTRODUCTION

Target damage produced by low  $L/D$  impactors (thin penetrators,  $L/D < 1$ ) is of interest with respect to the ballistic behavior of explosively driven plates. Such impactors were examined and tested by numerous researchers, [e.g., 1, 2]. The main aspect studied was the penetration capabilities of flat plates into a semi-infinite target. In the present study we consider a more general case of collision of low  $L/D$  curved impactors with target plates of finite thickness. Two main damage modes should be taken into account for this case: tensile failure (spall) caused by interaction of the rarefaction waves, and compressive failure caused by intense shear flow. As the  $L/D$

ratio decreases, spall failure tends to become the dominant damage mode for targets of finite thickness.

Spall phenomena are usually studied in planar impact tests (both the impactor and the target are plane-parallel; impactor-target misalignment does not exceed 0.5 mrad) characterized by an accurate uni-axial strain loading [3]. Here we present an analysis of the effects of non-planar (curvature) impactor on the spall and damage characteristics of a planar target. Since the flow generated in the target by such loading is obviously two-dimensional, it is analyzed by employing AUTODYN™ 2-D numerical simulations.

## EXPERIMENTAL SET-UP

Three types of 6061-T6 aluminum impactors were tested, as shown in Figure 1. The impactors were produced using CNC turning machin, from aluminum rod, to ensure well defined surfaces. The impactors were glued to a hollow aluminum sabot (Fig. 1). The constant radii of curvature ( $\mathcal{R}$ ) were hold with excellent,  $\pm 3$  mm, accuracy throughout all machined surfaces of each impactor. The thickness of the central part of all the impactors (including the plane parallel one) was about  $5 \pm 0.1$  mm. The projectiles, the sabots with glued impactors in the front, were accelerated using a 58-mm gas gun up to velocities of about  $600 \pm 20$  m/s. The exact experimental configurations (radius of curvature and impact velocity) are outlined in Table 1.

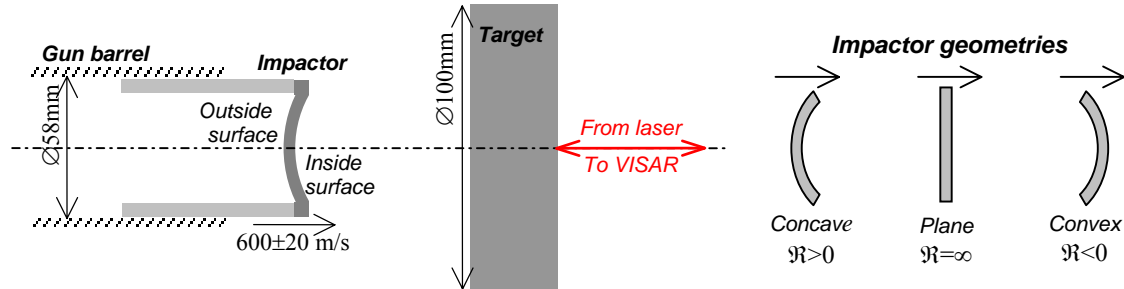


Figure 1 – left: Schematic view of the impact test set-up, and right: the projectiles

The targets were 20mm thick, 100mm diameter disks made of 6061-T6 aluminum. The projectile/target misalignment did not exceed 0.5 mrad in all the experiments. The

velocity of the rear surface of the target, Fig. 1, was continuously monitored by VISAR [4]. The VISAR measurements are presented in Fig. 2. It is interesting to note that by changing the radius of curvature of the impactor from concave to convex, the particle velocity of the back of the target decreases while the pulse duration increases. We'll refer to these observations later, while explaining the importance of these results.

Table 1 – Performed test matrix

Shot #	Impact Type	Impactor Radius of Curvature [mm]	Impact Velocity [m/s]
I	Planar	$\infty$	619
II	Concave	300 (360*)	578
III		260 (300)	597
IV		190 (250)	590
V		155 (160)	588
VI		Convex	-360 (-350)
VII	-155 (-155)		585

\* In parenthesis – Curvature radius of the impactor free surface

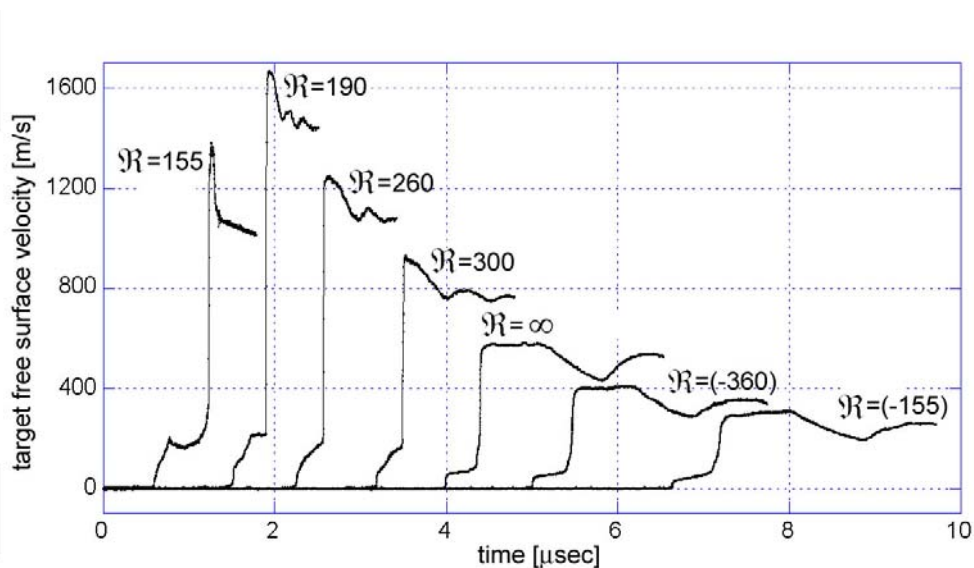


Figure 2 – VISAR records of the target free surface velocity, after the impact of 5-mm thickness impactors of different radii of curvature, at 600-m/s.

## NUMERICAL MODELING

Numerical simulations of the impact experiments were conducted employing AUTODYN-2D™ Lagrangian solver [5]. The modeling of Al6061-T6 was based on the Shock EOS, the Steinberg-Guinan strength model [6] and two immediate failure thresholds – principal stress for spallation ( $\sigma_{sp} = 1.8$  GPa) and shear strain for failure ( $\epsilon_f = 0.8$ ). Material erosion was used for numerical purposes of mesh stability and based upon geometric strain threshold equal to 3.0.

The material models were first validated by comparing the simulation results with the VISAR record for the target free surface velocity and the spallation failure aftermath of the planar impact test (shot I). Good agreement between the numerical and the experimental results were found for all the different impactor curvature (Fig. 3).

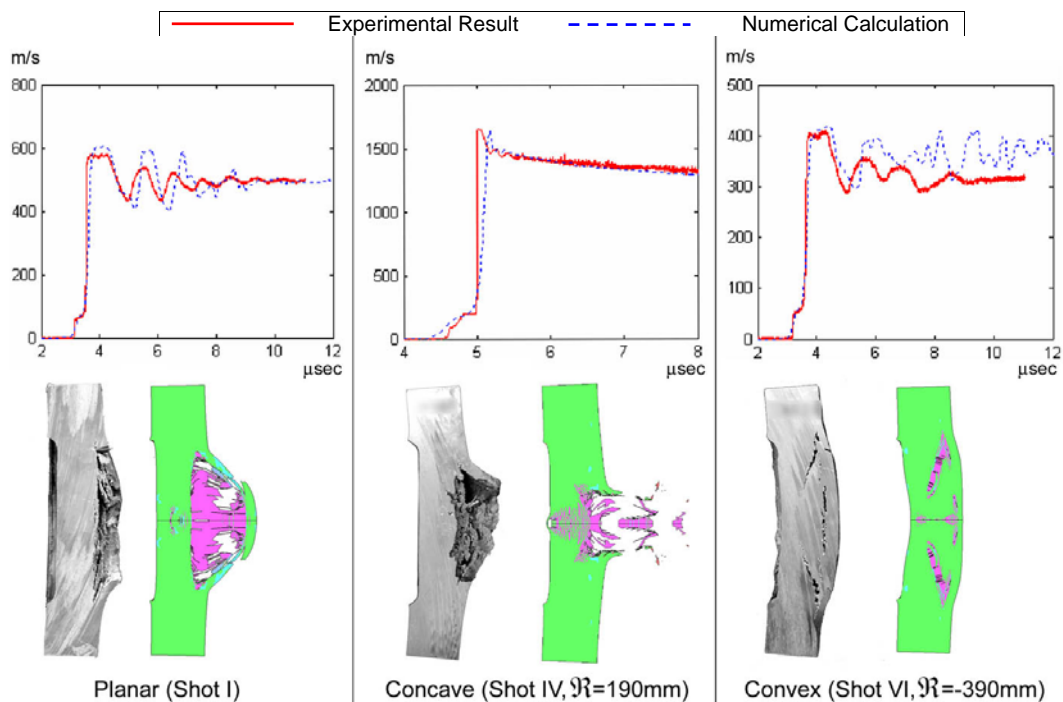


Figure 3 – Comparison between the experimental and the numerical results for the three impact cases. Top: Target free surface velocity; Bottom: Target post-mortem morphology (for numerical results at 500 μs).

The small discrepancies between the experimental and the numerical results are common for such simulations and originated mainly from the simplified constitutive models of the material. Nevertheless, these discrepancies do not affect our main results.

As apparent from Figures 2 and 3, the maximum target surface velocity achieved in the planar impact, about 600 m/s, is close to the impact velocity. The maximum target surface velocity achieved in the concave test is more than twice that of the planar test, while in the convex tests the maximum target velocities were lower than that of the planar impact. In all the experiments the velocity of the spall scab is about 70 m/s lower than the maximum velocity of the target surface.

## NUMERICAL ANALYSIS

A parametric numerical analysis was conducted. For a given impactor geometry (impactor radius  $R_0$ , thickness  $L$ , and radius of curvature  $\mathfrak{R}$ ) and projectile velocity a series of numerical calculations with different target thickness was conducted. Such calculation series yielded the maximum target thicknesses  $T_{spall}$  at which the spall fragments are detached from the target material. Varying the  $R_0/\mathfrak{R}$  ratio yields the dependence  $T_{spall}/L$  ( $R_0/\mathfrak{R}$ ) shown in Fig. 4.

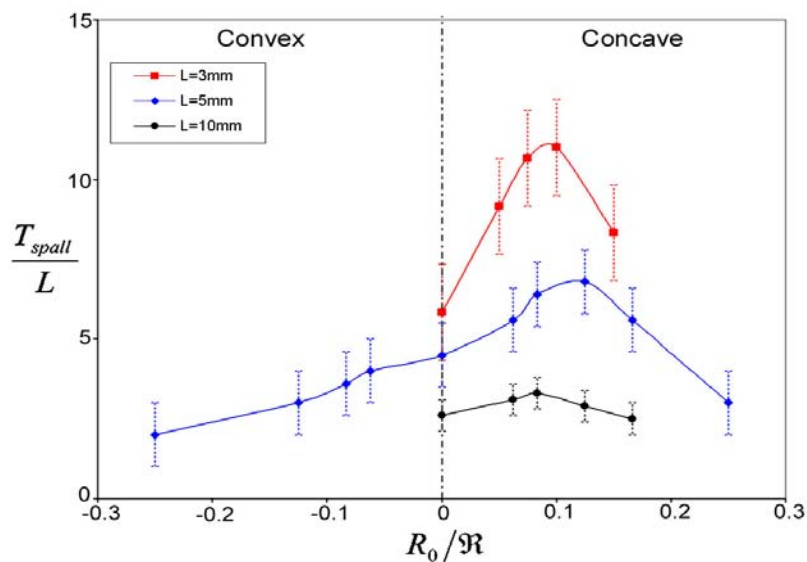


Figure 4 – Maximum target thickness vs. the radius of curvature of the impactors ( $v_0=600\text{m/s}$ ,  $R_0=25\text{mm}$ )

As apparent from this figure, such dependencies have distinct maxima whose positions are shifted slightly by varying the impactor thickness  $L$ . It also comes out, as can be seen in Fig. 2, shot IV, that the spall scab (plate) of the thickest target has the highest kinetic energy per unit mass.

## DISCUSSION

The shock wave structures created in the same target by three types of impactors are presented in Fig. 5. The converging and the diverging character of the shock waves generated by the concave and the convex impactors, respectively, are clearly seen.

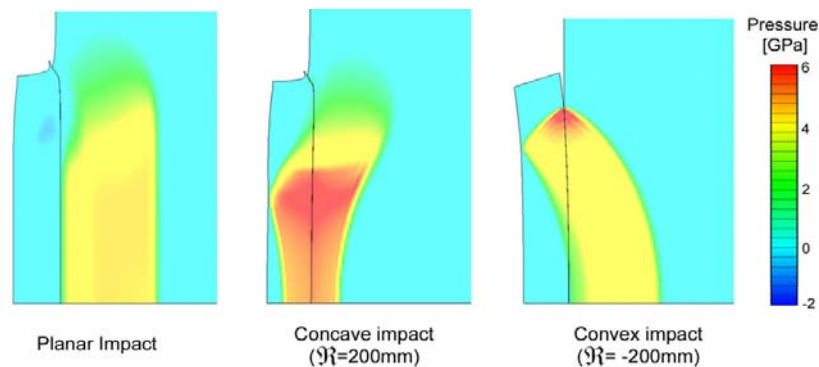


Figure 5 – The shock front induced in the target by three different types of impactors, 2  $\mu$ sec after first impactor-target contact (numerical results,  $v_0=600$  m/s,  $R_0=25$ mm)

Since the materials of the impactor and the target are the same the particle velocity behind the shock front generated in the target by planar impact is about half the impact velocity. After reflection of the shock front from the rear target surface the particle velocity of the surface jumps by a factor of two and gets close to the impact velocity (see Fig. 3).

Spall failure in planar impact tests is initiated by the tensile stress generated by the interference of two release waves arriving from the free surfaces of the impactor and the target. If this tensile stress (generated at a definite target plane) exceeds the material tensile strength a spall fracture occurs. Separation of the spalled scab from the target is determined by the scab kinetic energy, i.e. by the scab volume and by its final (post-spall) velocity. The former is determined by the depth and the area of the surface where the spall threshold conditions were obtained while the latter is determined by the amplitude of the compressive shock.

In the case of planar impact the spall occurs simultaneously at a plane where the two release-waves meet. This plane is parallel to the impactor (as well as to the target) surface, the thickness of the spall scab is the depth of the spall site, and the area (or the radius) of the spall scab is established by the arrival of the release waves from the periphery of the impactor-target contact area. These geometrical parameters determine the scab volume while the scab velocity may be estimated (in the case of the same impactor and target material) as the impact velocity with the deduction of half velocity pullback, as explained above.

As was found, both experimentally and numerically, the departure of the impactor shape from the plane-parallel one, changes both the scab volume and its velocity. Hence, explanation of the  $T_{\text{spall}}$  maxima of Fig. 4 requires understanding the nature of the compressive shock generated by impactors of different curvatures.

The damage scenario in the case of the curved impact differs from that of the planar impact but the final result is also determined by the sequence of the shock and release events. The  $x$ - $t$  diagrams presented in Fig. 6 depicts the different compression-tension timing in three impact configurations: planar, concave and convex. The various colors in this figure present the wave structure and the pressure level, in Eulerian coordinates (unlike a Lagrangian  $x$ - $t$  diagram, moving upwards, and keeping  $x$  coordinate constant, we do not follow a given particle).

It is clearly seen that in the vicinity of the spall site the duration of the compressive part of the loading cycle in the convex case is slightly longer than in the planar impact but it is shortened later on by the early release arrival from periphery of the curved impactor.

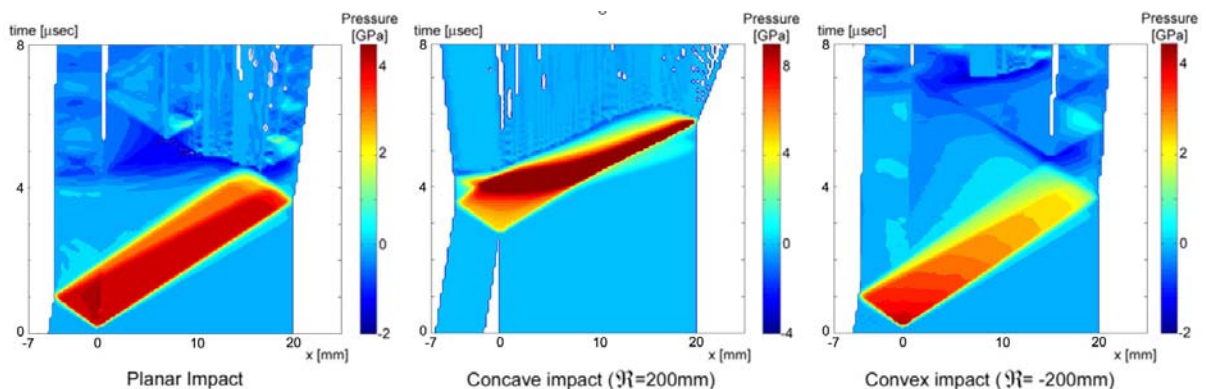


Figure 6 –  $x$ - $t$  diagrams of pressure dynamics along the impact axis of symmetry for three different impact cases, for 20mm finite thickness target ( $v_0=600$  m/s,  $R_0=25$ mm)

Examining Fig. 6, an immediate result can be obtained. The velocity of the shock wave entering the target is quite different in the three cases, the fastest one being in the concave case, and as it is well known, this means that in this case we also have the strongest shock wave, as can also be seen in the strong colors in the pressure contours. This observation will be addressed in the following sections.

It should also be noted that the curved impactor may serve as a source of additional release waves, unlike the planar case. From the moment the first impactor-target touch (at the center, when the impactor is convex, or in the periphery, when it is concave) the phase velocity, the propagation velocity of the impactor-target contact surface, is responsible of a continuous generation of the compressive waves. Depending on the impact velocity, on the target speed of sound and on the local impactor-target inclination (impactor curvature), the phase velocity may be supersonic or subsonic. If the phase velocity is subsonic, an unloading wave may be generated at the contact edge [7] interfering with the previously generated compressive signal. The change from supersonic to subsonic phase velocity determines the so called: the "effective" impacted area. This effect can be seen in Fig. 6, for the two curved impactors, by examining the location of the deep (red) color position. This unloading affects the location as well as the velocity of the scab.

### **Concave impactor**

The use of concave impactors (impactor radius of curvature  $\mathfrak{R}>0$ ) results in the amplification of the compressive stress (and, respectively, of the particle velocity) in the vicinity of the axis of the impactor-target system. The highest velocity of the target surface that is obtained in this case (see velocity profile  $\mathfrak{R}=190\text{mm}$  in Fig. 2) is related to two contradictory wave effects, as will be explained hereby. Focusing the converging shock wave, as seen in the x-t diagram in Fig. 6 (Note! the pressure scale of the central diagram of Fig. 6 is twice the scale of the left and right diagrams) requires simultaneous arrival of the compressive signals from the impactor periphery and from the impactor center at some point at the target surface.

Due to geometry, the release wave traveling from the impactor periphery arrives at this point much earlier than the release wave from the impactor center. In the case of thin impactor and large difference between the propagation speeds of compressive and release waves the peripheral release wave can overrun the compressive signals responsible for the stress amplification. As a result, the peripheral release can halt the amplification and even lead to a decrease of the stress amplitude.

The duration of the velocity profiles, as seen in Figs. 2 and 6, apparently decreases with the decrease of the impactor radius of curvature; the fast decay of the velocity profile of the  $\mathfrak{R}=155\text{mm}$  configuration is, possibly, both "defocused" and suppressed by hydrodynamic decay. In the case of the surface-focused impact (impactor radius of



curvature is equal to say;  $\mathcal{R}$ s) the velocity of the spall scab will be the highest one. The mass of the scab, however, will be minimal: the spall surface is very close to the target surface and the spall conditions are achieved at a limited area (clearly seen in the central diagram of Fig. 6). In order to increase the scab kinetic energy the depth of the spall site and its area should be increased. This can be achieved by increasing the impactor radius of curvature  $\mathcal{R}$  (increasing the effective area) with respect to  $\mathcal{R}$ s. Such increase, however, has a limitation: the amplification of the stress at the "focusing" plan will be smaller by the premature passage of the peripheral release wave. This amplification-release "competition" yields the maxima on the  $T_{\text{spall}}$  dependencies of Fig. 4.

### Convex impactor

In the case of the convex impactor ( $\mathcal{R} < 0$ ) the flow in the target is apparently divergent. Propagation of the divergent compressive wave front through the target results in the decrease of the wave amplitude with the propagation distance, as can be also seen in Fig. 6. This is true both for the elastic precursor and for the plastic waves as can clearly be seen in the Fig. 2 (profiles with  $\mathcal{R} = \infty$ ,  $\mathcal{R} = -360\text{mm}$ , and  $\mathcal{R} = -155\text{mm}$ ). As in any impact, the tensile stress in the target appears as a result of interference of two release waves. However, in the case of the convex impactor the duration of the release waves arriving at the spall site from the peripheral parts of the impactor is increased: the first release signal arrives from the center after a time interval equal to that of the planar impact ( $\mathcal{R} = \infty$ ) while the last release signal arrives from the impactor perimeter. The voids whose coalescence is responsible for the spall fracture have therefore longer time for their growth and may do that at lower stress. As a result the effective tensile rate (the slope of the unloading part of the pulse following the compressive plateau in Fig. 2) that precedes the spall failure in the convex experiments is lower than that in the planar impact, and consequently, the apparent spall stress in these shots is lower. The final outcome is that in this case we have a longer and lower tension wave resulting in thinner target thickness  $T_{\text{spall}}$ .

### SUMMARY

Target spallation induced by low  $L/D$  impactors of different curvature and thickness was studied experimentally and numerically. Simple modeling of the material failure in the numerical simulations, calibrated using planar impact experiments, enables us to analyze the material flow due to the loading and unloading shock waves in the target and in the impactor.

As can be seen from the numerical and the experimental results, the spall characteristics and the critical thickness for spall detachment are strongly affected by the curvature of the impactor. Concave impactors cause superposition of the impact-induced shock, which, with the effect of the rarefaction timing, leads to maximization, at a certain impactor curvature, of the scab velocity and its critical thickness. The divergent shock generated by convex impactors is weakened with the propagation distance and, therefore, leads to a spall that is characterized by decreased kinetic energy of the scab.

Quantitative analysis of the effects observed for the concave impact will be presented in the near future.

### ACKNOWLEDGMENT

The work is partially supported by the Basic Research Fund of the Israeli Ministry of Defense within the framework of Project No. 84297-501.

### REFERENCES

- [1] J.D. Walker, *Int. J. Impact Engng*, **23**, 957-966 (1999)
- [2] D.L. Orphal, C.E. Anderson Jr., R.R. Franzen, J.D. Walker, P.N. Schneidwind and M.E. Majerus, *Int. J. Impact Engng*, **14**, 551-560 (1993)
- [3] A. Tarabay, L. Seaman, D.R. Curran, G.I. Kanel, S.V. Rasorenov, A.V. Utkin, *Spall Fracture*, Springer, 2003.
- [4] L. M. Barker, and R. E., J. Hollenbach, *J. Appl. Phys.*, **43**, 4669-4675 (1972).
- [5] AUTODYN™ – ver. 6.1 Document Library, Century Dynamics Inc. (2005)
- [6] D.J. Steinberg, S.J. Cochran and M.W. Guinan, *J. Appl. Phys.*, **51**, 1498-1504 (1980).
- [7] S.K. Godunov, A.A. Deribas, A.V. Zabrodin, and N.S. Kozin, Hydrodynamic effects in colliding solids, *J. Comp. Phys*, 5 (N3), 517-539, 1970.